Natural optical activity and its control by electric field in electrotoroidic systems

Sergey Prosandeev, Andrei Malashevich, Zhigang Gui, Lydie Louis, Raymond Walter, Ivo Souza, and L. Bellaiche

Phys. Rev. B **87**, 195111 — Published 9 May 2013

DOI: 10.1103/PhysRevB.87.195111

Natural optical activity and its control by electric field in electrotoroidic systems

Sergey Prosandeev[1,2], Andrei Malashevich[3], Zhigang Gui[1],
Lydie Louis[1], Raymond Walter[1], Ivo Souza[4] and L. Bellaiche[1]
[1]*Physics Department,University of Arkansas, Fayetteville, Arkansas 72701, USA*
[2]*Institute of Physics, South Federal University, Rostov on Don, Russia, 344090*
[3]*Department of Applied Physics, Yale University,*
New Haven, Connecticut 06511, USA
[4]*Centro de Física de Materiales (CSIC) and DIPC,*
Universidad del País Vasco, 20018 San Sebastián,
and Ikerbasque Foundation, 48011 Bilbao, Spain

(Dated: April 22, 2013)

Abstract

We propose the existence, via analytical derivations, novel phenomenologies, and first-principles-based simulations, of a new class of materials that are not only spontaneously optically active, but also for which the sense of rotation can be switched by an electric field applied to them– via an induced transition between the dextrorotatory and laevorotatory forms. Such systems possess electric vortices that are coupled to a spontaneous electrical polarization. Furthermore, our atomistic simulations provide a deep microscopic insight into, and understanding of, this class of naturally optically active materials.

I. INTRODUCTION

The speed of propagation of circularly-polarized light traveling inside an *optically active* material depends on its helicity[1,2]. Accordingly, the plane of polarization of linearly polarized light rotates by a fixed amount per unit length, a phenomenon known as *optical rotation*. One traditional way to make materials optically active is to take advantage of the Faraday effect, by applying a magnetic field. However, there are some specific systems that are *naturally gyrotropic*, that is they spontaneously possess optical activity. Examples of known natural gyrotropic systems are quartz[3], some organic liquids and aqueous solutions of sugar and tartaric acid[1], the $Pb_5Ge_3O_{11}$ compound[4,5], and the layered crystal $(C_5H_{11}NH_3)_2ZnCl_4$[6]. Finding novel natural gyrotropic materials has great fundamental interest. It may also lead to the design of novel devices, such as optical circulators and amplifiers, especially if the *sign* of the optical rotation can be efficiently controlled by an external factor that is easy to manipulate.

When searching for new natural gyrotropic materials, one should remember the observation of Pasteur that chiral crystals display spontaneous optical activity, which reverses sign when going from the original structure to its mirror image[7]. Hence it is worthwhile to consider a newly discovered class of materials that are potentially chiral, and therefore may be naturally gyrotropic. This class is formed by electrotoroidic compounds (also called ferrotoroidics[8]). These are systems that possess an electrical toroidal moment, or equivalently, exhibit electric vortices[9]. Such intriguing compounds were predicted to exist around nine years ago[10], and were found experimentally only recently[11–15]. One may therefore wonder if this new class of materials is indeed naturally gyrotropic, and/or if there are other necessary conditions, in addition to the existence of an electrical toroidal moment, for such materials to be optically active.

In this work, we carry out analytical derivations, original phenomenologies and first-principles-based computations that successfully address all the aforementioned important issues. In particular, we find that electrotoroidic materials do possess spontaneous optical activity, but only if their electric toroidal moment changes *linearly* under an applied electric field. This linear dependence is further proved to occur if the electrotoroidic materials also possess a spontaneous electrical polarization that is coupled to the electric toroidal moment, or if they are also piezoelectric with the strain affecting the value of the electric toroidal

moment. We also find that, in the former case, the applied electric field further allows the control of the sign of the optical activity. Our atomistic approach also reveals the evolution of the microstructure leading to the occurrence of field-switchable gyrotropy, and shows that the optical rotatory strength can be significant in some electrotoroidic systems.

II. RELATION BETWEEN GYROTROPY AND ELECTRICAL TOROIDAL MOMENT IN ELECTROTOROIDIC SYSTEMS

Let us first recall that the gyrotropy tensor elements, g_{ml}, are defined via[16]:

$$g_{mk} = \frac{\omega}{2c} e_{ijm} \gamma_{ijk} \tag{1}$$

where e_{ijm} is the Levi-Civita tensor[17], c is the speed of light, and ω is the angular frequency. Note that this angular frequency is not restricted to the optical range. For instance, it can also correspond to the 1-100 GHz frequency range. The γ tensor provides the linear dependence of the dielectric permittivity on the wave vector $\mathbf{k}$ in the optically active material, that is:

$$\varepsilon_{ik}(\omega, \mathbf{k}) = \varepsilon_{ik}^{(0)}(\omega) + i\gamma_{ikl} k_l \tag{2}$$

Here, k_l is the l-component of the wave vector; $\varepsilon_{ik}(\omega, \mathbf{k})$ denotes the double Fourier transform in time and space of the dielectric tensor, with the long-wavelength components being denoted by $\varepsilon_{ik}^{(0)}$. Throughout this manuscript we adopt Einstein notation, in which one implicitly sums over repeated indices (as it happens, e.g., for the l index in Eq. (2)).

Thus, the calculation of the gyrotropy tensor can be reduced to the calculation of the tensor γ responsible for the spatial dispersion of the dielectric permittivity.

Alternatively, one can use the following formula for the dielectric permittivity[1,16]:

$$\varepsilon_{ik}(\omega, \mathbf{k}) = \delta_{ik} + \frac{4\pi i}{\omega} \sigma_{ik}(\omega, \mathbf{k}) = \delta_{ik} + \frac{4\pi i}{\omega} (\sigma_{ik}^{(0)}(\omega) + \sigma_{ikl} k_l) \tag{3}$$

where δ_{ik} is the Kronecker symbol and $\sigma_{ik}(\omega, \mathbf{k})$ is the effective conductivity tensor in the reciprocal space, at a given frequency[1]. σ_{ikl} is the third-rank tensor associated with the linear dependence of the effective conductivity tensor on the wave vector, and $\sigma_{ik}^{(0)}$ is the effective conductivity tensor at zero wave vector. Combining Eqs. (3) with Eq. (2) yields:

$$\gamma_{ikl} = \frac{4\pi}{\omega} \sigma_{ikl} = \frac{4\pi}{\omega} (\sigma_{ikl}^{S}(\omega) + \sigma_{ikl}^{A}(\omega)) \tag{4}$$

where

$$\sigma^A_{ijk} = \frac{1}{2}(\sigma_{ijk} - \sigma_{jik}) \tag{5}$$

and

$$\sigma^S_{ijk} = \frac{1}{2}(\sigma_{ijk} + \sigma_{jik}) \tag{6}$$

Moreover, using the results of Ref.[18] and working at nonabsorbing frequencies (i.e., frequencies, such as GHz in ferroelectrics, for which the corresponding energy is below the band gap of the material), one can write

$$\sigma^A_{ijk} = ic\,(e_{jkl}\beta_{il} - e_{ikl}\beta_{jl}) + \omega\xi_{ijk} \tag{7}$$

with

$$\beta_{ij} = i\mathrm{Im}(\chi^{em}_{ij}) = -i\mathrm{Im}(\chi^{me}_{ji}) \tag{8}$$

and

$$\xi_{ijk} = \frac{1}{2}\left[\frac{dQ_{kj}}{dE_i} - \frac{dQ_{ki}}{dE_j}\right] \tag{9}$$

where Im stands for the imaginary part and Q is the quadrupole moment of the system[19]. χ^{me} is the response of the magnetization, $\mathbf{M}$, to an electric field $\mathbf{E}$, while χ^{em} is the response of the electrical polarization, $\mathbf{P}$, to a magnetic field $\mathbf{B}$, that is:

$$\chi^{me}_{ij} = \frac{dM_i}{dE_j} \quad \text{and} \quad \chi^{em}_{ji} = \frac{dP_j}{dB_i} \tag{10}$$

Inserting Eq. (7) into Eq. (4) provides :

$$\gamma_{ijk} = \frac{4\pi}{\omega}\left[c\left(e_{jkl}\mathrm{Im}\,\chi^{me}_{li} - e_{ikl}\mathrm{Im}\,\chi^{me}_{lj}\right) + \omega\xi_{ijk}\right] + \gamma^S_{ijk} \tag{11}$$

where $\gamma^S_{ijk} = (4\pi/\omega)\sigma^S_{ijk}$ is the contribution of the symmetric part of the conductivity to the γ tensor. As a result, γ^S_{ijk} is non-zero only when the system is magnetized or possesses a spontaneous magnetic order[16].

Let us now focus on the magnetization, which can be written as[19]:

$$\mathbf{M} = \frac{1}{2cV}\int (\mathbf{r} \times \mathcal{J}(\mathbf{r}))\, d^3r \tag{12}$$

where c is the speed of light, V is the volume of the system, $\mathbf{r}$ is the position vector, and $\mathcal{J}(\mathbf{r})$ is the current density. We consider here the following contributions to this density:

$$\mathcal{J}(\mathbf{r}) = \dot{\mathcal{P}}(\mathbf{r}) + c\ \boldsymbol{\nabla} \times \mathcal{M}_{\mathbf{0}}(\mathbf{r}) \tag{13}$$

where the dot symbol refers to the partial derivative with respect to time. $\mathcal{P}(\mathbf{r})$ is the polarization *field*, that is, the quantity for which the spatial average is the macroscopic polarization. Similarly, $\mathcal{M}_{\mathbf{0}}(\mathbf{r})$ is the magnetization field, that is, the quantity for which the spatial average is the part of the macroscopic magnetization that does not originate from the time derivative of the polarization field[20]. By plugging this latter equality into Eq. (12), we have:

$$\mathbf{M} = \frac{1}{2cV}\int \left(\mathbf{r} \times \dot{\mathcal{P}}(\mathbf{r})\right) d^3r + \frac{1}{2V}\int \left(\mathbf{r} \times \boldsymbol{\nabla} \times \mathcal{M}_{\mathbf{0}}(\mathbf{r})\right) d^3r = \frac{1}{2cV}\int \left(\mathbf{r} \times \dot{\mathcal{P}}(\mathbf{r})\right) d^3r + \mathbf{M}_0 \tag{14}$$

The analytical expression of this latter equation bears some similarities with the definition of the electrical toroidal moment, $\mathbf{G}$, that is[9]

$$\mathbf{G} = \frac{1}{2V}\int \left(\mathbf{r} \times \mathcal{P}(\mathbf{r})\right) d^3r \quad , \tag{15}$$

More precisely, taking the time derivative of $\mathbf{G}$ gives:

$$\dot{\mathbf{G}} \simeq \frac{1}{2V}\int \left(\mathbf{r} \times \dot{\mathcal{P}}(\mathbf{r})\right) d^3r \tag{16}$$

when omitting the time dependency of the volume (the numerical simulations presented below indeed show that one can safely neglect this dependency when computing the time derivative of the electric toroidal moment).

As a result, combining Eq. (16) and Eq. (14) for a monochromatic wave having an ω angular frequency gives:

$$\mathbf{M} - \mathbf{M}_0 \simeq \frac{1}{c}\dot{\mathbf{G}} = -\frac{i\omega}{c}\mathbf{G} \tag{17}$$

in electrotoroidic systems.

Plugging this latter equation in Eq. (10) then gives:

$$\chi_{ij}^{me} = \chi_{ij}^{me(0)} - \frac{i\omega}{c}\frac{dG_i}{dE_j} \tag{18}$$

where $\chi_{ij}^{me(0)}$ is the magnetoelectric tensor related to the derivative of $\mathbf{M}_0$ with respect to an electric field. Therefore

$$\mathrm{Im}\left(\chi_{ij}^{me} - \chi_{ij}^{me(0)}\right) = -\frac{\omega}{c}\frac{dG_i}{dE_j} \tag{19}$$

This relation between the imaginary part of the magnetoelectric susceptibility and the field derivative of the electrical toroidal moment is reminiscent of the connection discussed in Ref.[22] between the linear magnetoelectric response and the *magnetic* toroidal moment.

Inserting Eqs. (19) and (9) into Eq. (11) then provides:

$$\begin{aligned}\gamma_{ijk} =&\gamma^S_{ijk} + \frac{4\pi c}{\omega}\left(e_{jkl}\mathrm{Im}\chi^{me(0)}_{li} - e_{ikl}\mathrm{Im}\chi^{me(0)}_{lj}\right)\\ &+4\pi\left[e_{ikl}\frac{dG_l}{dE_j} - e_{jkl}\frac{dG_l}{dE_i} + \frac{1}{2}\left(\frac{dQ_{kj}}{dE_i} - \frac{dQ_{ki}}{dE_j}\right)\right]\end{aligned} \tag{20}$$

Combining this latter equation with Eq. (1), and recalling that γ^S_{ijk} is a symmetric tensor while e_{ijm} is antisymmetric (which makes their product vanishing), gives:

$$\begin{aligned}g_{mk} =&4\pi\left(\delta_{mk}\mathrm{Im}\chi^{me(0)}_{ll} - \mathrm{Im}\chi^{me(0)}_{mk}\right)\\ &+\frac{4\pi\omega}{c}\left[\left(\frac{dG_m}{dE_k} - \frac{dG_l}{dE_l}\delta_{mk}\right) + \frac{1}{4}e_{ijm}\left(\frac{dQ_{kj}}{dE_i} - \frac{dQ_{ki}}{dE_j}\right)\right]\end{aligned} \tag{21}$$

Choosing a specific gauge[20] and neglecting quadrupole moments (simulations reported below show that spontaneous and field-induced quadrupole moments can be neglected for the ferrotoroidics numerically studied in Section IV) lead to the reduction of Eq. (21) to:

$$g_{mk} = \frac{4\pi\omega}{c}\left[\left(\frac{dG_m}{dE_k} - \frac{dG_l}{dE_l}\delta_{mk}\right)\right] \tag{22}$$

This formula nicely reveals that optical activity should happen when electrical toroidal moment *linearly* responds to an applied electric field.

III. NECESSARY CONDITIONS FOR GYROTROPY IN ELECTROTOROIDIC SYSTEMS

According to Eq. (22), an electrotoroidic system possessing non-vanishing derivatives of its electrical toroidal moment with respect to the electric field automatically possesses natural optical activity. Let us now prove analytically that the occurrence of such non-vanishing derivatives requires additional symmetry breaking in electrotoroidic systems, namely that an electrical polarization or/and piezoelectricity should also exist, as well as couplings between electrical toroidal moment and electric polarization and/or strain.

For that, let us express the free energy of an electrotoroidic system that exhibits couplings between electrical toroidal moment $\mathbf{G}$, polarization $\mathbf{P}$, and strain η as:

$$F = F_0 + \zeta_{ijkl}G_iG_j\eta_{kl} + \lambda_{ijkl}G_iG_jP_kP_l + q_{ijkl}P_iP_j\eta_{kl} - h_iG_i \tag{23}$$

where $h_i = (\boldsymbol{\nabla}\times\mathbf{E})_i$ is the field conjugate of G_i.

The equilibrium condition, $\partial F/\partial G_n = 0$, implies that

$$\partial F_0/\partial G_n + (\zeta_{njkl} + \zeta_{jnkl})G_j\eta_{kl} + (\lambda_{njkl} + \lambda_{jnkl})G_jP_kP_l = h_n \tag{24}$$

which indicates that h_n depends on both the polarization and strain.

As a result, the change in electrical toroidal moment with electric field can be separated into the following two contributions:

$$\frac{d\mathrm{G_i}}{d\mathrm{E_j}} = \left(\frac{dG_i}{dE_j}\right)^{(1)} + \left(\frac{dG_i}{dE_j}\right)^{(2)} \tag{25}$$

with

$$\left(\frac{dG_i}{dE_j}\right)^{(1)} = \frac{dG_i}{dh_n}\frac{\partial h_n}{\partial P_l}\frac{dP_l}{dE_j} = \chi_{in}^{(G)}\frac{\partial h_n}{\partial P_l}\chi_{lj}^{(P)} \tag{26}$$

and

$$\left(\frac{dG_i}{dE_j}\right)^{(2)} = \frac{dG_i}{\partial h_n}\frac{\partial h_n}{\partial \eta_{kl}}\frac{d\eta_{kl}}{dE_j} = \chi_{in}^{(G)}\frac{\partial h_n}{\partial \eta_{kl}}d_{klj} \tag{27}$$

Here

$$\chi_{in}^{(G)} = \frac{dG_i}{dh_n} \tag{28}$$

is the response of the electrical toroidal moment to its conjugate field,

$$\chi_{ij}^{(P)} = \frac{dP_i}{dE_j} \tag{29}$$

is the electric susceptibility, and

$$d_{ijk} = \frac{d\eta_{ij}}{dE_k} \tag{30}$$

is a piezoelectric tensor.

The remaining derivatives appearing in Eqs. (26) and (27) can be found from Eq. (24):

$$\left(\frac{\partial h_n}{\partial P_l}\right) = (\lambda_{njlm} + \lambda_{njml} + \lambda_{jnlm} + \lambda_{jnml})G_jP_m \tag{31}$$

and

$$\left(\frac{\partial h_n}{\partial \eta_{kl}}\right) = (\zeta_{njkl} + \zeta_{jnkl})G_j \tag{32}$$

Equations (25)-(32) reveal that there are two scenario for the occurence of natural optical activity in electrotoroidic systems. In the first scenario, the system possesses a finite polarization that has a bilinear coupling with the electrical toroidal moment (see Eqs. (26), (31), and (23)). In the second scenario, the electrotoroidic system is also piezoelectric, and electrical toroidal moment and strain are coupled to each other (see Eqs. (27), (32), and

(23)). An example of the latter can be found in Reference[23], where a pure gyrotropic phase transition leading to a piezoelectric, but non-polar, $P2_12_12_1$ state (that exhibits spontaneous electrical toroidal moments) was discovered in a perovskite film. Next, we describe the theoretical prediction of a material where the former scenario is realized.

IV. PREDICTION AND MICROSCOPIC UNDERSTANDING OF GYROTROPY IN ELECTROTOROIDIC SYSTEMS

The system we have investigated numerically is a nanocomposite made of periodic squared arrays of $BaTiO_3$ nanowires embedded in a matrix formed by (Ba,Sr)TiO_3 solid solutions having a 85% Sr composition. The nanowires have a long axis oriented along the [001] pseudo-cubic direction (chosen to be the z-axis). They possess a squared cross-section of 4.8x4.8 nm^2 in the (x,y) plane, where the x- and y-axes are chosen along the pseudo-cubic [100] and [010] directions, respectively. The distance (along the x- or y-directions) between adjacent $BaTiO_3$ nanowires is 2.4 nm.

We choose this particular nanocomposite system because a recent theoretical study[24], using an effective Hamiltonian ($H_{\rm eff}$) scheme, revealed that its ground state possesses a spontaneous polarization along the z-direction inside the whole composite system, as well as electric vortices in the (x,y) planes inside each $BaTiO_3$ nanowire, with the same sense of vortex rotation in every wire. Such a phase-locking, ferrotoroidic and polar state is shown in Fig. 1a. It exhibits an electrical toroidal moment being parallel to the polarization. Figure 1a also reveals the presence of antivortices located in the *medium*, half-way between the centers of adjacent vortices.

In the present study, we use the same $H_{\rm eff}$ as in Ref.[24], combined with molecular dynamics techniques, to determine the response of this peculiar state to an *ac* electric field applied along the main, z-direction of the wires. In our simulations, the amplitude of the field was fixed at 10^9 V/m and its frequency ranged between 1GHz and 100GHz. The sinusoidal frequency-driven variation of the electric field with time makes therefore this field ranging in time between 10^9 V/m (field along [001]) and -10^9 V/m (field along [00-1]). The idea here is to check if the electrical toroidal moment has a *linear* variation with this field at these investigated frequencies, and therefore if the investigated system can possess nonzero gyrotropy coefficients (see Eq.(22)).

In this effective Hamiltonian method, developed in Ref.[25] for (Ba,Sr)TiO_3 (BST) compounds, the degrees of freedom are: the local mode vectors in each 5-atom unit cell (these local modes are directly proportional to the electric dipoles in these cells), the homogeneous strain tensor and inhomogeneous-strain-related variables[26]. The total internal energy contains a local mode self-energy, short-range and long-range interactions between local modes, an elastic energy and interactions between local modes and strains. Further energetic terms model the effect of the interfaces between the wires and the medium on electric dipoles and strains, as well as take into account the strain that is induced by the size difference between Ba and Sr ions and its effect on physical properties. The parameters entering the total internal energy are derived from first principles. This H_{eff} can be used within Monte-Carlo or Molecular dynamics simulations to obtain finite-temperature static or dynamical properties, respectively, of relatively large supercells (i.e., of the order of thousands or tens of thousands of atoms). Previous calculations[25,27–30] for various disordered or ordered BST systems demonstrated the accuracy of this method for several properties. For instance, Curie temperatures and phase diagrams, as well as the subtle temperature-gradient-induced polarization, were well reproduced in BST materials. Similarly, the existence of two modes (rather than a single one as previously believed for a long time) contributing to the GHz-THz dielectric response of pure $BaTiO_3$ and disordered BST solid solutions were predicted via this numerical tool and experimentally confirmed.

Figures 2(a) and 2(b) report the evolution of the z-component of the electrical toroidal moment, G_z, and of the polarization, P_z, respectively, as a function of the electric field, for a frequency of 1GHz at a temperature of 15K. In practice, G_z is computed within a lattice model[24], by summing over the electric dipoles located at the lattice sites rather than by continuously integrating the polarization field of Eq. (15) over the space occupied by the nanowires. The panels in Fig. 1 show snapshots of important states occurring during these hysteresis loops, in order to understand gyrotropy at a microscopic level. A striking piece of information revealed by Fig. 2 (a) is that G_z *linearly decreases* with a slope of -1.6 e/V when the applied *ac* field varies between 0 (state 1) and its maximum value of 10^9 V/m (state 2). Such variation therefore results in *positive* g_{11} and g_{22} gyrotropy coefficients that are both equal to 0.94×10^{-7} for a frequency of 1GHz, according to Eq. (22) (that reduces here to $g_{11} = g_{22} = -\frac{\omega}{c\varepsilon_0}\frac{dG_z}{dE}$ in S.I. units, since there are no x- and y-components of the toroidal moment and since the field is applied along z in the studied case). Interestingly,

we found that the aforementioned slope of -1.6 e/V stays roughly constant over the entire frequency range we have investigated (up to 100GHz). As a result, Eq. (22) indicates that $g_{11} = g_{22}$ should be proportional to the angular frequency ω of the applied *ac* field, and that the meaningful quantity to consider here is the ratio between g_{11} and this frequency. Such ratio is presently equal to 5.9×10^{-16} per Hz. Moreover, the rate of optical rotation is related to the product between ω/c and the gyrotropy coefficient according to Ref.[16]. As a result, the rate of optical rotation depends on the *square* of the angular frequency because of Eq. (22), as consistent with one finding of Biot in 1812[2]. Here, the ratio of the rate of optical rotation to the square of the angular frequency is found to be four orders of magnitude larger than that measured in "typical" gyrotropic materials, such as $Pb_5Ge_3O_{11}$[4,5]. As a result, the plane of polarization of light will rotate by around 1.2 radians per meter at 100GHz (or by 1.24×10^{-4} radians per meter at 1GHz), when passing through the system.

Figure 2b indicates that the observed decrease of G_z is accompanied by an increase of the polarization, which is consistent with our numerical finding that increasing the field from 0 to 10^9 V/m reduces the x- and y-components of the electric dipoles inside the nanowires (that form the vortices) while enhancing the z-component of the electric dipoles in the whole nanocomposite (i.e., wires and medium). Interestingly, the antivortices in the medium progressively disappear during this linear decrease of G_z and increase of P_z, as shown in Figs 1. Figures 2 also show that decreasing the electric field from 10^9 V/m (state 2) to $\simeq$ -0.031 $\times$ 10^9 V/m (state 3) leads to a linear increase of the electric toroidal moment (yielding the aforementioned values of g_{11} and g_{22}), while the z-component of the polarization decreases but still stay positive.

Further increasing the magnitude of negative electric fields up to $\simeq$ -0.094 $\times$ 10^9 V/m results in drastic changes for the microstructure: dipoles in the medium now adopt negative z-components (state 3), then sites at the interfaces between the medium and the wires also flip the sign of the z-component of their dipoles (states 3 and α). During these changes, the overall polarization rapidly varies from a significant positive value along the z-axis to a slightly negative value (Fig. 2b), while G_z is nearly constant, therefore rendering the gyrotropic coefficients null. Then, continually increasing the strength of the negative *ac* field up to $\simeq$ -0.48 $\times$ 10^9 V/m leads to the next stage: dipoles *inside* the wires begin to change the sign of their z-components (states β, 4 and γ) until all of the z-components of these dipoles point down (state 5). During that process, P_z becomes more and more negative,

while the electrical toroidal moment decreases very fast but remains positive (indicating that the chirality of the wires is unaffected by the switching of the overall polarization).

Once this process is completed, further increasing the magnitude of the applied field along $[00\bar{1}]$ up to -10^9 V/m (state $2'$), leads to a *linear decrease* of the electrical toroidal moment. Interestingly, this decrease is quantified by a slope dG_z/dE that is exactly *opposite* to the corresponding one when going from state 1 to state 2. As a result, the g_{11} and g_{22} gyrotropic coefficients associated with the evolution from state 5 to state $2'$ are now *negative* and equal -0.94×10^{-7} at 1GHz.

Finally, Figures 1 and 2 indicate that varying now the *ac* field from its minimal value of -10^9 V/m to its maximal value of 10^9 V/m leads to the following succession of states: $2'$, 5, $1'$, $3'$, α', β', $4'$, γ', $5'$ and 2, where the $'$ superscript used to denote the i$'$ states (with i=2, 3, 4, 5, α, β and γ) indicates that the corresponding states have z-components of their dipoles that are all opposite to those of state i (for instance, state β' has z-components of the dipoles being positive in the medium while being negative in the wires, as exactly opposite to state β). During this path from state $2'$ to state 2, the gyrotropic coefficients g_{11} and g_{22} can be negative (from state $2'$ to state $3'$) or positive (from state $5'$ to state 2), depending on the sign of the polarization.

Such possibility of having both negative and positive gyrotropic coefficients in the same system originates from the fact that the polarization can be down or up, and is consistent with Eqs. (31), (26) and (22). As a result, one can turn the polarization of light either in clockwise or anticlockwise manner in electrotoroidic systems, via the control of the direction of the polarization by an external electric field – which induces the switching between the dextrorotatory and laevorotatory forms of these materials (see states 1 and $1'$). Such control may be promising for the design of original devices[31,35].

Figure 3 shows how the gyrotropic coefficient g_{11} depends on temperature. One can clearly see that g_{11} significantly increases as the temperature increases up to 240K. As indicated in the figure, the temperature behavior of g_{11} is very well fitted by $A/\sqrt{(T_C - T)(T_G - T)}$, where A is a constant, $T_C = 240K$ is the lowest temperature at which the polarization vanishes and $T_G = 330K$ is the lowest temperature at which the electric toroidal moment is annihilated[24]. In order to understand such fitting, let us combine Eqs (22), (26) and (31)

for the studied case, that is:

$$g_{11} = -\frac{4\pi\omega}{c}\frac{dG_3}{dE_3} = -\frac{4\pi\omega}{c}\chi_{3n}^{(G)}\frac{\partial h_n}{\partial P_l}\chi_{l3}^{(P)} = -\frac{4\pi\omega}{c}(\lambda_{n3l3} + \lambda_{n33l} + \lambda_{3nl3} + \lambda_{3n3l})\chi_{3n}^{(G)}G_3P_3\chi_{l3}^{(P)} \tag{33}$$

The usual temperature dependencies of the order parameter and its conjugate field imply that G_3 and P_3 should be proportional to $\sqrt{(T_G - T)}$ and $\sqrt{(T_C - T)}$, respectively, while their responses, $\chi_{3n}^{(G)}$ and $\chi_{l3}^{(P)}$, should be proportional to $1/(T_G - T)$ and $1/(T_C - T)$, respectively. This explains why the behavior of g_{11} as a function of T is well described by $A/\sqrt{(T_C - T)(T_G - T)}$.

V. SUMMARY

In summary, we propose the existence of a new class of spontaneously optically active materials, via the use of different techniques (namely, analytical derivations, phenomenologies and first-principles-based simulations). These materials are electrotoroidics for which the electric toroidal moment changes linearly under an applied electric field. Such linear change is demonstrated to occur if at least one of the following two conditions is satisfied: (1) the electric toroidal moment is coupled to a spontaneous electrical polarization; or (2) the electric toroidal moment is coupled to strain and the whole system is piezoelectric. We also report a realization of case (1), and further show that applying an electric field in such a case allows a systematic control of the sign of the optical rotation, via a field-induced transition between the dextrorotatory and laevorotatory forms. We therefore hope that our study deepens the current knowledge of natural optical activity and will be put in use to develop novel technologies.

This work is financially supported by ONR Grants N00014-11-1-0384 and N00014-08-1-0915 (S.P. and L.B.), ARO Grant W911NF-12-1-0085 (Z.G. and L.B.), NSF grant DMR-1066158 (L.L. and L.B.). I.S acknowledges support by Grant MAT2012-33720 from the Spanish Ministerio de Economía y Competitividad. S.P. appreciates Grant 12-08-00887-a of Russian Foundation for Basic Research. L.B. also acknowledges discussion with scientists sponsored by the Department of Energy, Office of Basic Energy Sciences, under contract

ER-46612, Javier Junquera and Surendra Singh.

[1] D. B. Melrose and R. C. McPhedran, *Electromagnetic Processes in Dispersive Media* (Cambridge University Press, Cambridge, 1991).

[2] L. D. Barron, *Molecular Light Scattering and Optical Activity* (Cambridge University Press, Cambridge, 2004).

[3] D. F. J. Arago, Mém. Inst. **12**, Part I, 93 (1811).

[4] J. P. Dougherty, E. Sawaguchii, and L. E. Cross, Appl. Phys. Lett. **20**, 364 (1972).

[5] C. Konak, V. Kopsky and F. Smutny, J. Phys. C: Solid State Phys. **11**, 2493 (1978).

[6] A. Gómez Cuevas, J. M. Pérez Mato, M. J. Tello, G. Madariaga, J. Fernández, López Echarri, F. J. Zuñiga, and G. Chapuis Phys. Rev. B **29**, 2655 (1984).

[7] L. Pasteur Researches on the Molecular Asymmetry of Natural Organic Products (Edinburg: Alembic 1897).

[8] H. Schmid, J. Phys.: Condens. Matter **20**, 434201 (2008).

[9] V. M. Dubovik and V. V. Tugushev, Physics Reports **187**, 145 (1990).

[10] I. I. Naumov, L. Bellaiche, and H. Fu, Nature **432**, 737 (2004).

[11] A. Gruverman, D. Wu, H-J Fan, I. Vrejoiu, M. Alexe, R. J. Harrison, and J. F. Scott, J. Phys.: Condens. Matter. **20**, 342201 (2008).

[12] R. G. P. McQuaid, L. J. McGilly, P. Sharma, A. Gruverman, and A. Gregg, Nat Commun. **2**, 404 (2011).

[13] N. Balke, B. Winchester, W. Ren, Y. H. Chu, A. N. Morozovska, E. A. Eliseev, M. Huijben, R. K. Vasudevan, P. Maksymovych, J. Britson, S. Jesse, I. Kornev, R. Ramesh, L. Bellaiche, L. Q. Chen, and S. V. Kalinin Nature Physics, **8**, 81 (2012).

[14] R. K. Vasudevan, Y. C. Chen, H. H. Tai, N. Balke, P. Wu, S. Bhattacharya, L. Q. Chen, Y. H. Chu, I. N. Lin, S. V. Kalinin, and V. Nagarajan, ACS Nano. **5**, 879 (2011).

[15] C. T. Nelson, B. Winchester, Y. Zhang, S. J. Kim, A. Melville, C. Adamo, C. M. Folkman, S. H. Baek, C. B. Eom, D. G. Schlom, L. Q. Chen, X. Pan, Nano Lett. **11**, 828 (2011).

[16] L. D. Landau, E. M. Lifshitz, and L. P. Pitaevskii, Electrodynamics of Continuous Media, Second Edition: Volume 8 (Course of Theoretical Physics), (Elsevier, New-York 1984).

[17] J. R. Tyldesley, An introduction to Tensor Analysis: For Engineers and Applied Scientists.

(Longman, Niw-York 1973).

[18] A. Malashevich, and I. Souza, Phys. Rev. B **82**, 245118 (2010).

[19] R. E. Raab, and O. L. De Lange, *Multipole Theory in Elecromagnetism.* (Clarendon Press - Oxford 2005).

[20] Note that $\mathcal{P}(\mathbf{r})$ and $\mathcal{M}_{\mathbf{0}}(\mathbf{r})$ are technically ill-defined in the sense that they depend on the choice of a gauge[21]. However, all the different gauges result in the same current density, $\mathcal{J}(\mathbf{r})$,[21] which is the physical quantity that appears in Eqs. (12) and (13). As a result, the choice of the gauge does not modify our results, in general, and Eq. (21), in particular. Such conclusion can also be reached by realizing that the quantity appearing in the left hand side of Eq. (12) is the *macroscopic* magnetization, and as such, should not depend on the choice of a gauge. Note, however, that Eq. (22) is deduced from Eq. (21) via the annihilation of all the contributions stemming from $\mathbf{M}_0$. As a result, a specific choice of gauge was made in going from Eq.(21) to Eq.(22), namely the "P-only" gauge discussed in Ref.[21].

[21] L.L. Hirst, Reviews of Modern Physics, **69**, 607 (1997).

[22] N. A. Spaldin, M. Fiebig, and M. Mostovoy, J. Phys. Cond. Mat. **20**, 434203 (2008).

[23] S. Prosandeev, I. A. Kornev, L. Bellaiche, Phys. Rev. Lett. **107**, 117602 (2011).

[24] L. Louis, I. Kornev, G. Geneste, B. Dkhil, and L. Bellaiche, J. Phys. Cond. Mat. **24**, 402201 (2012).

[25] L. Walizer, S. Lisenkov, and L. Bellaiche, Phys. Rev. B **73**, 144105 (2006).

[26] W. Zhong, D. Vanderbilt, and K. M. Rabe, Phys. Rev. B **52**, 6301 (1995).

[27] N. Choudhury, L. Walizer, S. Lisenkov, and L. Bellaiche, Nature **470**, 513 (2011).

[28] S. Lisenkov, and L. Bellaiche, Phys. Rev. B **76**, 020102(R) (2007).

[29] J. Hlinka, T. Ostapchuk, D. Nuzhnyy, J. Petzelt, P. Kuzel, C. Kadlec, P. Vanek, I. Ponomareva, and L. Bellaiche, Phys. Rev. Lett. **101**, 167402 (2008).

[30] Q. Zhang, and I. Ponomareva, Phys. Rev. Lett. **105**, 147602 (2010).

[31] Note that Eq. (23) involves the *squares* of the toroidal moment and of the polarization for the coupling interaction between these two physical quantities. As a result, one can easily understand that the presently studied nanocomposite has a ground state that is four times degenerated, due to the fact that the polarization and electrical toroidal moment can independently be parallel or antiparallel to the z-axis. These four states have the same probability (of 25%) to occur when cooling the system from high to low temperature. In our simulations, when the system

statistically chooses one of these states below the critical temperature, it stays in it when further decreasing the temperature, likely because the potential barrier to go from one of these states to the other three states is too high. Moreover, one can also force the system to be in one of these four states by applying, and then removing, the conjugate fields of the polarization and electrical toroidal moment. For instance, the selection of the states for which the polarization is parallel to the z-axis requires the application of an homogeneous electric field along [001]. Similarly, obtaining states with electrical toroidal moment being aligned along [001] can be done by applying specific curled electric fields[32] (see also Refs.[9,33,34] for more details about how to control toroidal moments). Notice that creating a curled electric field along [001] can be practically realized by applying a magnetic field having a time derivative being oriented along $[00\bar{1}]$, since Maxwell equations directly relate the time derivative of a magnetic field with minus the curl of the electric field.

[32] Wei Ren and L. Bellaiche, Phys. Rev. Lett. **107**, 127202 (2011).

[33] S. Prosandeev, I. Ponomareva, I. Kornev, I. Naumov, and L. Bellaiche, Phys. Rev. Lett. **96**, 237601 (2006).

[34] S. Prosandeev, I. Ponomareva, I. Naumov, I. Kornev, and L. Bellaiche, Topical Review, J. Phys.: Condens. Matter **20**, 193201 (2008).

[35] Note that the homogeneous electric field is the field conjugate of the electrical polarization but is not the field conjugate of the electrical toroidal moment. As a result (and as proven by our simulations), applying an electric field can change the direction of the polarization but can not change the direction of the electrical toroidal moment. This explains why an electric field can control the chirality and optical activity in electrotoroidic systems.

Figure Captions.

FIG. 1. (color online) Dipole arrangement in the (x,y) plane of the studied nanocomposite for the states playing a key role in the occurrence of gyrotropy. The four wires are made of pure $BaTiO_3$, and the medium is mimicked to be formed by BST solid solutions having a 85% Sr composition. See text for the labels and meanings of the different panels.

FIG. 2 (color online) Predicted hysteresis loops in the studied nanocomposite at 15K, for a frequency of 1GHz. Panel (a) and (b) show the electrical toroidal moment and polarization, respectively, as a function of the value of the *ac* electric field. In these panels, the number and symbols inside parenthesis refer to the states displayed in FIG. 1.

FIG. 3. (color online) Temperature behavior of the g_{11} gyrotropic coefficient in the nanocomposite studied in the manuscript. The solid lines represent the fit of the data by $A/\sqrt{(T_C - T)(T_G - T)}$.

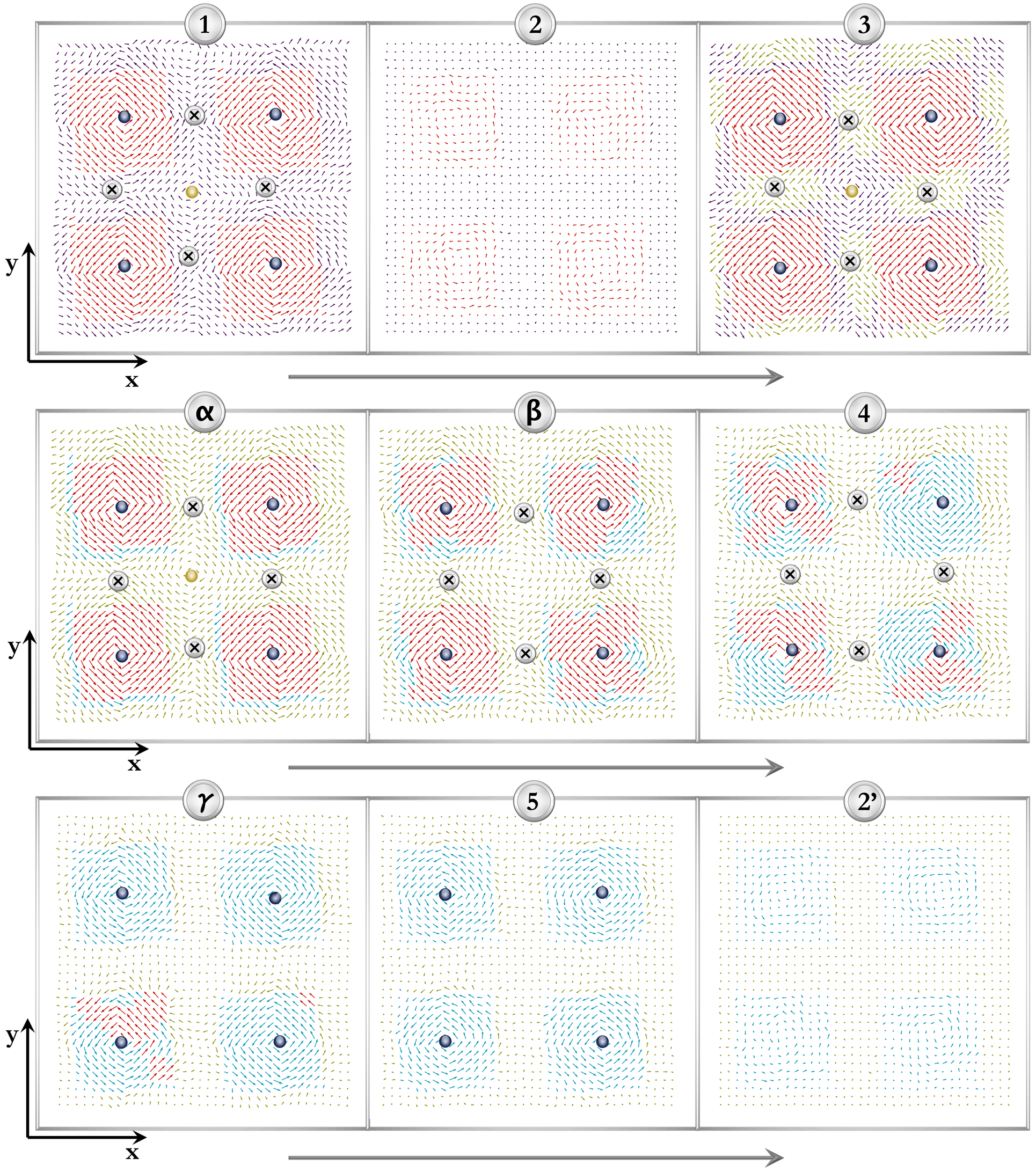

Legend

Arrows in wires

Positive dipole: z-direction (x,y) plane

Negative dipole: z-direction (x,y) plane

Arrows in matrix

Positive dipole: z-direction (x,y) plane

Negative dipole: z-direction (x,y) plane

Vortex in medium

Vortex in wire

Antivortex

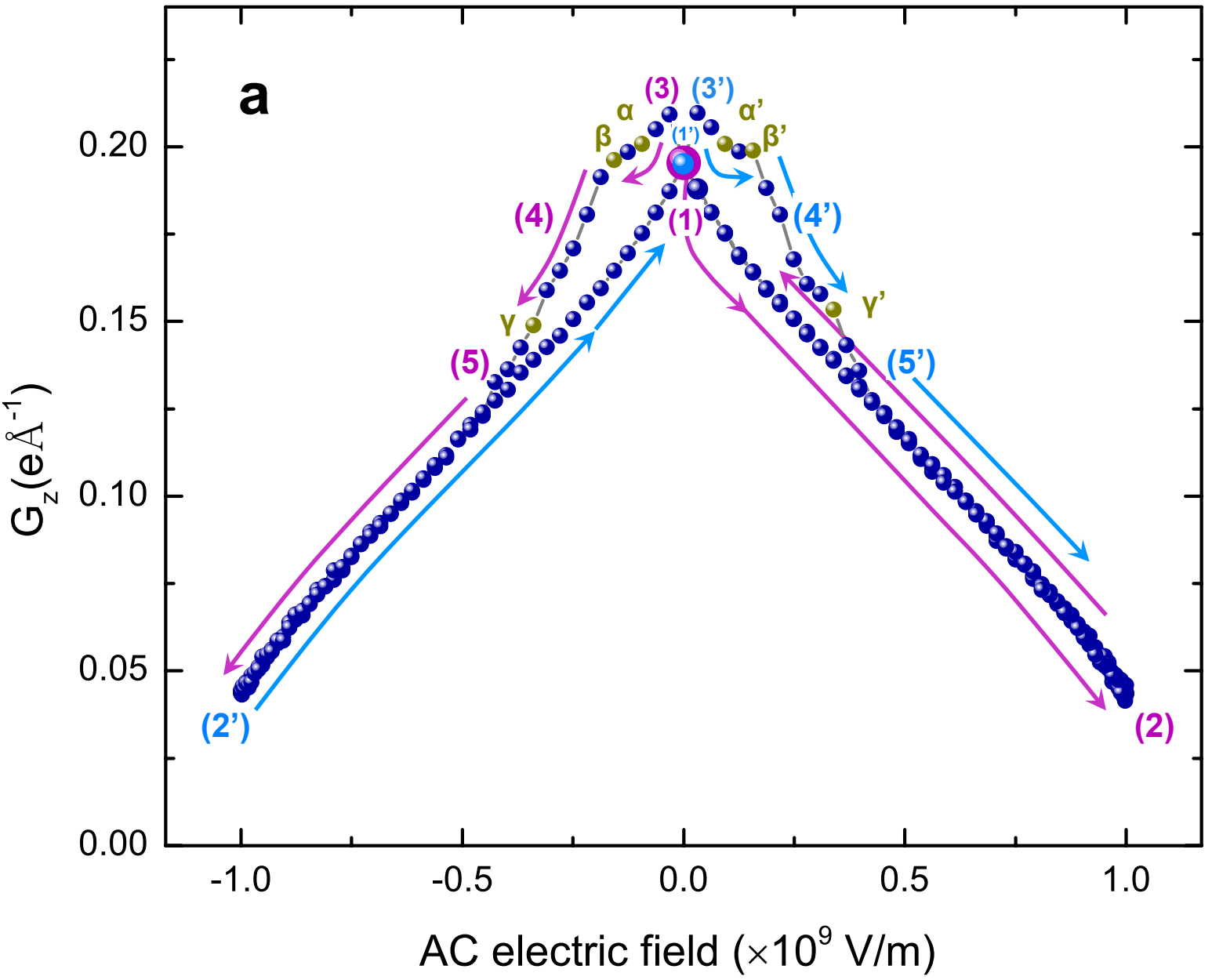
a
(3)
(3')
α
α'
β
β'
(1')
(4)
(1)
(4')
γ
γ'
(5)
(5')
(2')
(2)
0.20
0.15
0.10
0.05
0.00
G_z(eÅ^{-1})
-1.0
-0.5
0.0
0.5
1.0
AC electric field (×10^9 V/m)

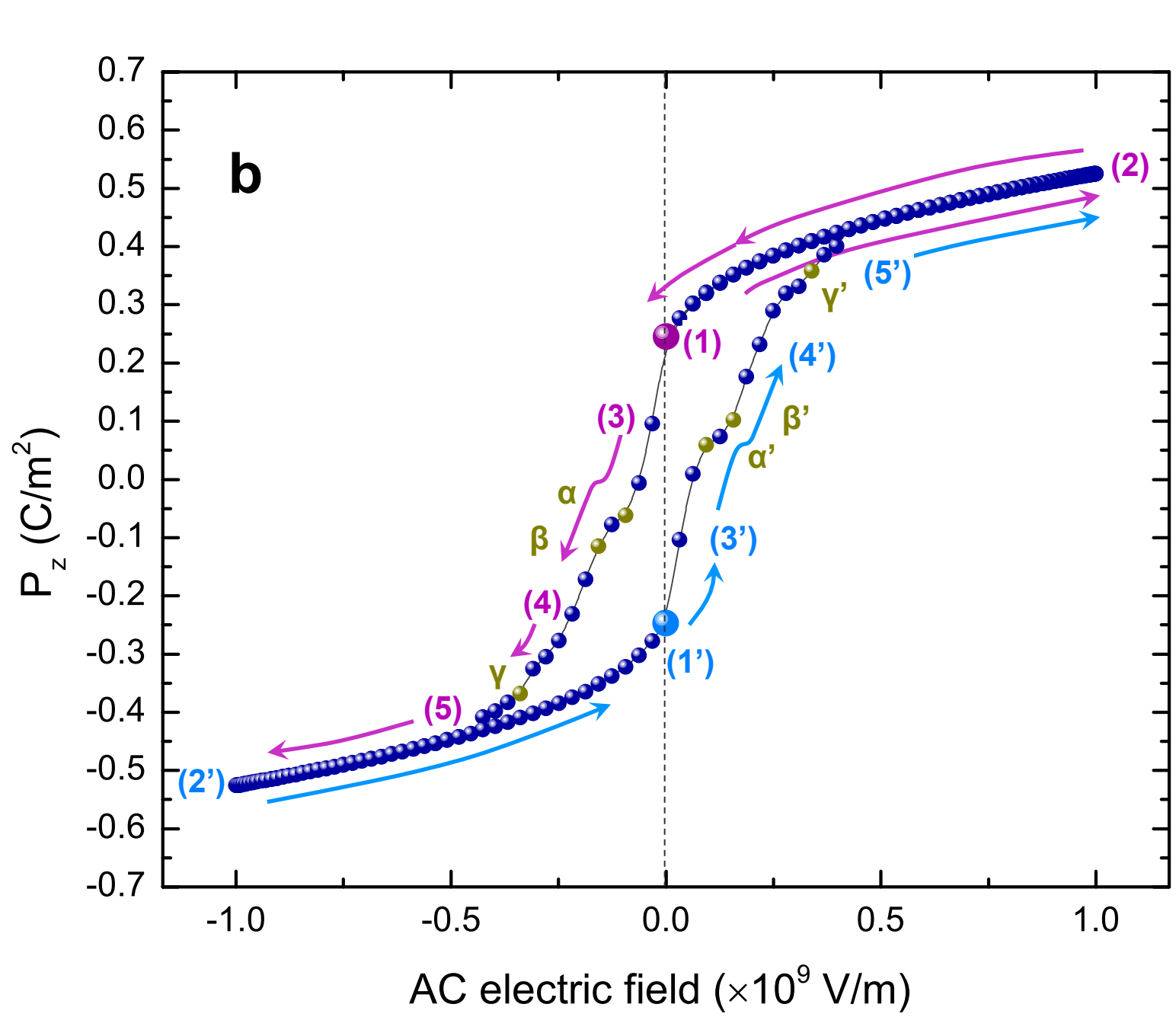
b
(2)
(5')
γ'
(1)
(4')
β'
α'
(3)
(3')
α
β
(4)
γ
(1')
(5)
(2')
0.7
0.6
0.5
0.4
0.3
0.2
0.1
0.0
-0.1
-0.2
-0.3
-0.4
-0.5
-0.6
-0.7
P_z (C/m^2)
-1.0
-0.5
0.0
0.5
1.0
AC electric field (×10^9 V/m)

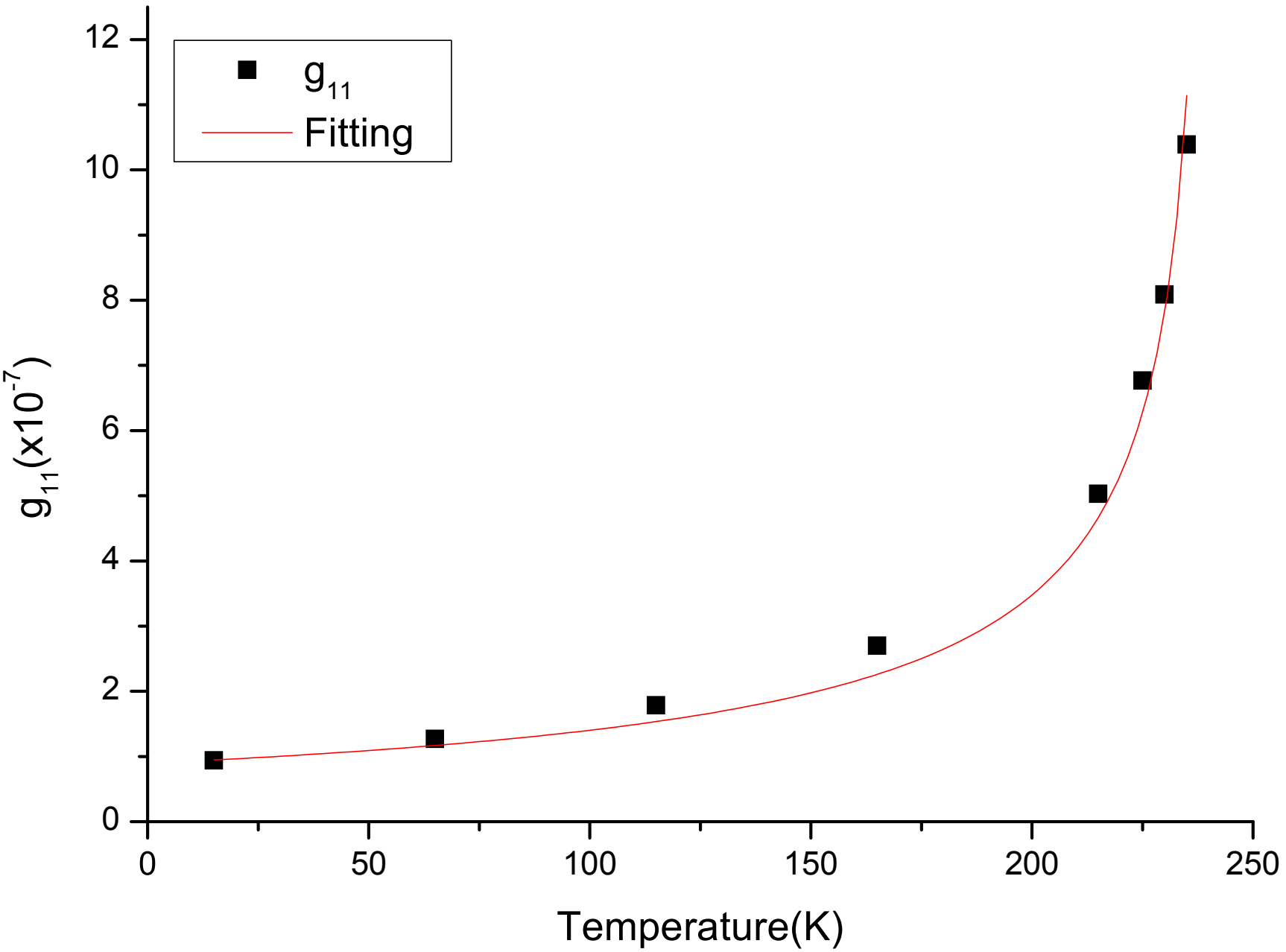
g11
Fitting
12
10
8
6
4
2
0
g11(x10-7)
0
50
100
150
200
250
Temperature(K)